ISSN 0965-545X, Polymer Science, Ser. A, 2014, Vol. 56, No. 6, pp. 907–916. © Pleiades Publishing, Ltd., 2014.

COMPOSITES

Conductivity and Dielectric Relaxation in Various Polyvinyl Alcohol/Ammonium Salt Composites[1]

Arbi Fattoum[a] and Mourad Arous[b]

[a] *Research Unit: Materials Environment and Energy (06/UR/12-01), Science Faculty Sidi Ahmed Zaroug 2112 Gafsa, Tunisia*

[b] *Laboratory of Composite Materials, Ceramics and Polymers, Physics Department, Science Faculty 3038 Sfax, Tunisia*

e-mail: arbi_fattoum@yahoo.fr, mouradarous@yahoo.fr

Received May 14, 2014;
Revised Manuscript Received August 12, 2014

Abstract—We studied electrical conductivity and dielectric relaxation in polyvinyl alcohol/ammonium chloride and polyvinyl alcohol/ammonium acetate composite films. Infrared absorbance showed the presence of H-bonding interaction between the salt and the polymer. X-ray diffraction showed the reduction of the grain size of ordered regions in the polymer matrix after adding salt. Thermo gravimetric analysis (TGA) showed water wt% content between 4.2 and 5.8%. Differential Scanning Calorimetry (DSC) showed the decrease of the glass transition due to retained water indicating its plasticizer effect. The ac conductivity studied in the frequency range from 10^{-1} Hz to 1 MHz and the temperature range from 10 to 150°C is described by the universal law of Jonsher characterizing the charge transport in disordered materials. With NH_4Cl inclusion, the dc conductivity showed a higher value in the vicinity of 4% but with $NH_4CH_3CO_2$ the dc conductivity decreases monotonically by increasing the salt amount. By using the dielectric permittivity and dielectric modulus we detected three relaxation processes which we attributed to electrode/sample polarization, alpha relaxation and conductivity relaxation respectively.

DOI: 10.1134/S0965545X14060145

INTRODUCTION

Ion-conducting polymer membranes have been widely investigated in the aim to be used in various chemical and electrochemical applications. As example, we cite diffusion dialysis, electrodialysis, electrolysis, rechargeable batteries and fuel cells [1, 2]. Researches aim to develop low-cost new materials endowed with good performances. Especially, enhanced ionic conductivity and good thermal and mechanical stabilities are key points of investigation in the field. According to literature relative to fuel cells and especially for low temperature type fuel cells, the electrolyte is generally made with polymer bearing sulfonate or carboxylate groups [3–6]. Sulfonate and carboxylate or other acid groups are used as sources of protons to ensure the electric conductivity by proton exchange processes. Proton conductivity is enhanced by the presence of humidity which ameliorates the proton exchange between the proton donor and water molecules. For this, in the fuel cell application the electrolyte is subjected to a humidification step prior to use. The retained water is distributed in the form of interconnected nanosized aqueous regions [6, 7].

In the present work, we chose the polyvinyl alcohol (PVA) as a polymer matrix. It is known by its hydrophilic properties, good transparency and fast charge transfer at electrode–electrolyte interface [8, 9]. This polymer has a high swelling property and thus provides the larger channels for transporting H^+ ions [7]. We realize the blending of PVA with ammonium chloride salt (NH_4Cl) or ammonium acetate salt ($NH_4CH_3CO_2$) used here as proton donors. We aim to investigate thermal, structural, conductivity and dielectric relaxation as a function of the salt amount in a temperature range which covers 80°C which is the habitual working temperature of polymer electrolyte fuel cells [10].

EXPERIMENTAL

Sample Preparation

We prepared PVA/NH_4Cl and PVA/$NH_4CH_3CO_2$ composites by using the solution cast method. In a first step, we dissolved the polyvinyl alcohol (99% hydrolyzed, Aldrich) in ultra pure water at 85°C. In a second step, we added the desired amount of ammonium salt to the solution with continuous stirring during two hours. We cast the obtained viscous solution on a Petri dish and we dried at ambient atmosphere during four days. This

[1] The article is published in the original.

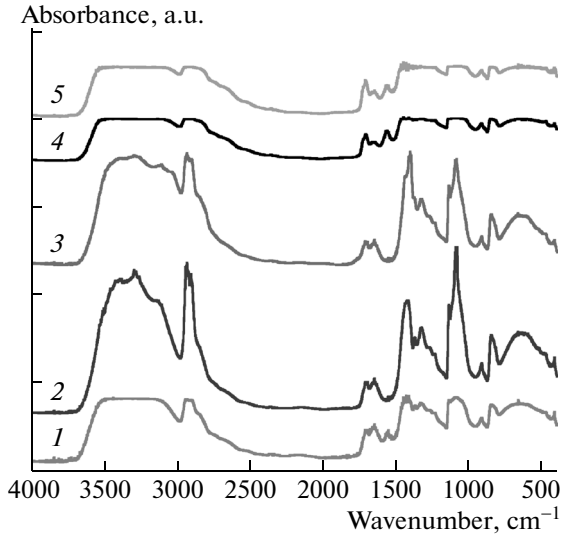

Fig. 1. IR absorbance of (*1*) pure PVA, (*2*) PVA/NH_4Cl 4%, (*3*) PVA/NH_4Cl 16%, (*4*) PVA/$NH_4CH_3CO_2$ 4%, and (*5*) PVA/$NH_4CH_3CO_2$ 12%.

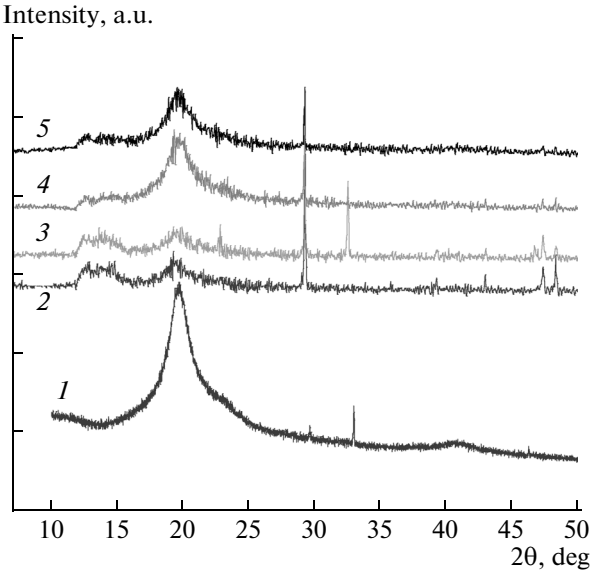

Fig. 2. XRD spectra of (*1*) pure PVA, (*2*) PVA/NH_4Cl 4%, (*3*) PVA/NH_4Cl 16%, (*4*) PVA/$NH_4CH_3CO_2$ 4%, and (*5*) PVA/$NH_4CH_3CO_2$ 12%.

method provided free standing films having 100 to 150 μm thickness, estimated by electron microscopy. We prepared two series of composite films with various amounts of ammonium salt corresponding to 4, 8, 12, and 16% of salt molar ratios.

Sample Characterization

We performed FTIR measurements in the range of 400–4000 cm^{-1} by using a Shimadzu 8400S spectrophotometer with a resolution of 2 cm^{-1}. We determined the weight loss by thermal gravimetric analysis (TGA) by using a SETSYS Evo (Setaram) thermal Analyzer from 20 to 400°C with a heating rate of 10°C/min. We effectuated Differential Scanning Calorimetry (DSC) by using a Perkin Elmer 4000 calorimeter from −30 to 300°C with a heating rate of 10°C/min to determine the glass transition temperature and other structural transformations. We conducted X-ray diffraction (XRD) by using an X'Pert Pro MPD diffractometer (Panalytical) to determine the variation of the crystalline structure as a function of the composition. For the electric study (conductivity and dielectric relaxation), we conducted dielectric measurements from 10 to 150°C by using a Novocontrol Alpha Analyzer in the frequency range of 0.1 Hz to 1 MHz. For this measurement, the film was sandwiched between two circular stainless steel electrodes related to a temperature controller. The measuring cell was immersed in pure nitrogen atmosphere and the sample was subjected to an alternative voltage of 50 mV amplitude.

RESULTS AND DISCUSSION

FTIR Measurements

We present in Fig. 1 infrared absorbance spectra of PVA matrix, PVA/NH_4Cl and PVA/$NH_4CH_3CO_2$ composites. We distinguish a large band around 3350 cm^{-1} attributed to O–H stretching, a peak around 2920 cm^{-1} assigned to C–H stretching, a peak around 1710 cm^{-1} due to C=O stretching [11, 12], a peak around 1430 cm^{-1} assigned to C–H vibration out of plane, a large band between 1100 and 1140 cm^{-1} assigned to C–H bending and C–O stretching [11, 9], a peak around 920 cm^{-1} due to O–H motion out of plane [13, 14]. All these peaks are also observed in composites spectra. In addition, we distinguish the appearance of a band around 3140 cm^{-1}, assigned to N–H absorption. We note also the progressive broadening of the band around 3300 cm^{-1} when we increase the salt amount. This behavior is more accentuated when PVA is blended with ammonium acetate salt. It is attributed to the presence of H-bonding interaction between the salt and the hydroxyl group of PVA.

XRD

We present in Fig. 2 X-Ray difractograms of various composites. We distinguish the characteristic peak of pure PVA around $2\theta = 19.6°$ [15]. This peak confirms the semi-crystalline structure of pure PVA: organized chain regions embedded in amorphous media. After the blending process, this peak remains located around the same 2θ position but becomes broader and

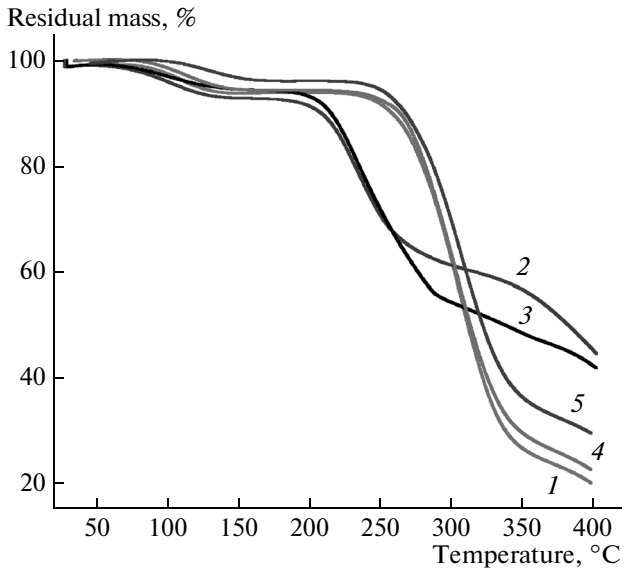

Fig. 3. TGA curves of (*1*) pure PVA, (*2*) PVA/NH_4Cl 4%, (*3*) PVA/NH_4Cl 16%, (*4*) PVA/$NH_4CH_3CO_2$ 4%, and (*5*) PVA/$NH_4CH_3CO_2$ 16%.

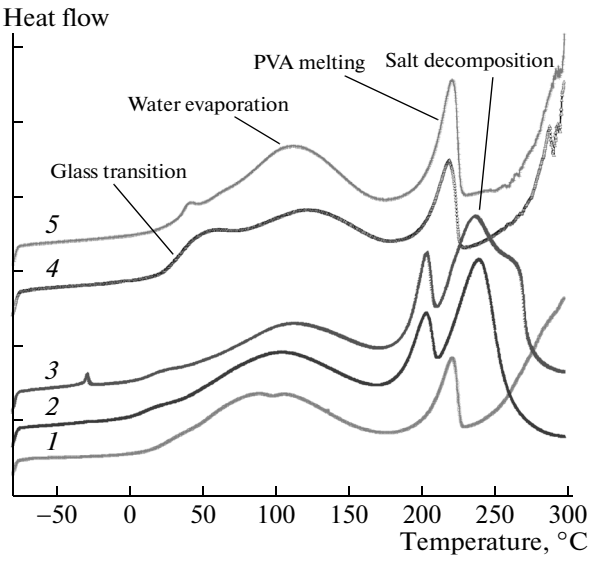

Fig. 4. (*1*) PVA, (*2*) PVA/NH_4Cl 4%, (*3*) PVA/NH_4Cl 16%, (*4*) PVA/$NH_4CH_3CO_2$ 4%, and (*5*) PVA/$NH_4CH_3CO_2$ 12%.

smaller in intensity. The amorphous structure is extended; the average grain size of the organized chain regions is reduced. We check the average particle size by using the Debye–Scherer formula [16]:

$$D = \frac{0.9\lambda}{B\cos\theta}, \quad (1)$$

where D designs the average diameter of the crystals, λ is the X-ray radiation wavelength and B is the peak full width at half maximum intensity. We find that B increases (i.e. the average diameter D decreases) by increasing the salt concentration in the composite.

Thermal Analyses

In TGA spectra (Fig. 3), we locate a first weight loss around 100°C attributed to water evaporation. From this loss we deduce the hydration wt % in each composite and its evolution versus the salt amount. In PVA/NH_4Cl, We find the highest amount of water in the 4% composite (Table 1). But in PVA/$NH_4CH_3CO_2$ this amount decreases monotonically when we increase the salt amount (Table 1). However, the two types of composites were prepared and dried in the same experimental conditions.

Also, we locate a second weight loss occurring around 228°C for pure PVA and between 236–241°C

Table 1. Water amount, glass transition, melting and degradation temperatures of various PVA/NH_4Cl and PVA/$NH_4CH_3CO_2$ composites

Sample	Salt, mol %	Water, wt %	T_g, °C	T_m, °C	T_{deg}, °C
Pure PVA	0%	4.95	24	219	228
PVA/NH_4Cl	4%	5.8	10	205	270
	8%	–	12	198	–
	12%	–	14	198	–
	16%	4.15	10	201	295
PVA/$NH_4CH_3CO_2$	4%	5.5	52	218	236
	8%	–	40	217	–
	12%	–	35	218	–
	16%	4.3	33	220	241

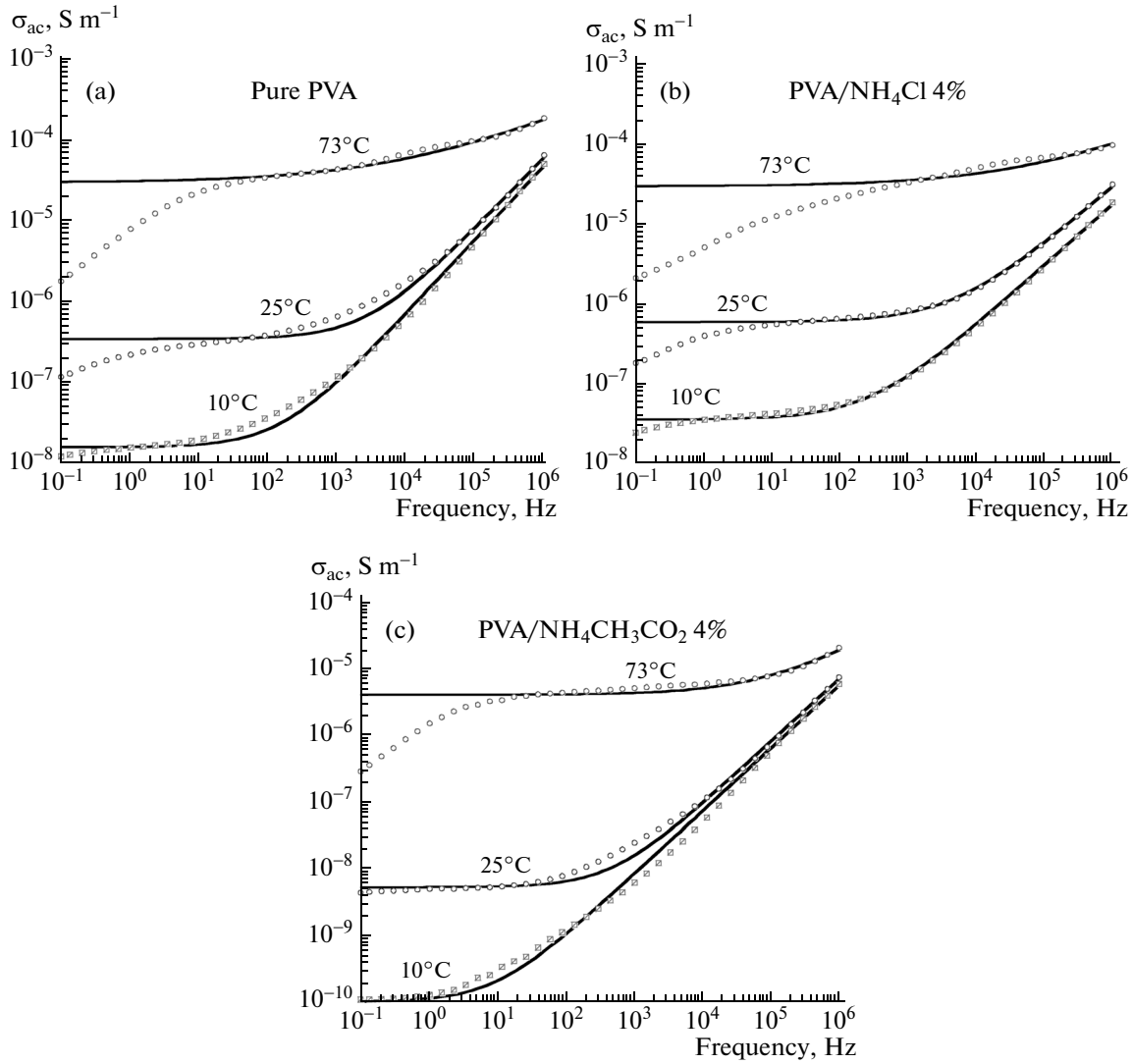

Fig. 5. Ac conductivity of (a) pure PVA, (b) PVA/NH_4Cl 4%, and (c) PVA/$NH_4CH_3CO_2$ 4% at 10, 25, and 73°C (solid lines are fitting curves to the universal Jonscher law).

for PVA/$NH_4CH_3CO_2$. This loss is attributed to PVA degradation. For PVA/NH_4Cl, the PVA degradation is observed around 270°C.

It is clear that thermal stability of the composite is enhanced by salt addition. The attractive hydrogen bonding between the salt molecules and the hydroxyl groups of the polymer which we confirmed by FTIR measurements enhances the thermal stability.

In DSC thermograms (Fig. 4), we locate an endothermic peak situated around 100°C. It corresponds to water evaporation. Also, we distinguish an endothermic peak corresponding to PVA melting, the melting temperature is noted T_m (Table 1). Also, we observe in all composite thermograms an endothermic peak corresponding to salt decomposition. Indeed, this peak doesn't appear in pure PVA thermogram.

Also, DSC spectra show an endothermic step corresponding to the glass/rubber transition temperature which we note T_g. The glass transition temperature is located around 24°C for pure PVA. This value is much lower than the $T_g = 86$°C of anhydrous PVA, available in literature [2]. Our result supports the plasticizer role played by retained water. For composites, the T_g is higher with $NH_4CH_3CO_2$ than with NH_4Cl (Table 1). This implies lower polymer chain mobility and confirms the role of the attractive interaction established between the salt and the polymer on the local mobility of the polymer chains.

Conductivity and Dielectric Relaxation

AC conductivity. We present in Figs. 5a, 5b, and 5c the alternative current conductivity $\sigma_{ac}(\sigma)$ for pure PVA, PVA/NH_4Cl 4% and PVA/$NH_4CH_3CO_2$ 4%

respectively. At low temperatures (around ambient temperature), curves are characterized by two frequency domains. The first is situated at low frequencies where the conductivity appears in the form of a plateau indicating frequency independent conductivity and a second region situated at higher frequencies where the conductivity varies as a power law ($A\omega^s$). The plateau defines the direct current conductivity noted σ_{dc}. The power law response signifies that conductivity in higher frequency is ensured by charge hopping processes, backward/forward hopping between localization states randomly distributed. This response is usually observed in disordered materials. We observe this behavior as well in the matrix as in composites with various amounts of ammonium salt. The conductivity is expressed by the universal Jonsher law [17]:

$$\sigma_{ac}(\omega, T) = \sigma_{dc}(T) + A(T)\omega^{s(\omega, T)}, \quad (2)$$

where T is the absolute temperature, A is a proportionality coefficient and s is the power law exponent lying between 0 and 1. We present in the same (Figs. 5a, 5b, and 5c) the fitting curves to the universal Jonsher law as solid lines.

As we increase temperature, the plateau corresponding to dc conductivity shifts towards higher frequencies and it appears a branch in which the conductivity decreases when the frequency decreases. This branch is due to charge accumulation at electrode/sample interfaces. The enhancement of the charge mobility due to increase of temperature accentuated the accumulation process and favors the capacitive behavior of the sample/electrode interface. The global response becomes dominated by this capacitive behavior at low frequencies and higher temperatures. We observed in literature similar conductivity behavior in ionic conducting systems analogous to ours [18].

3.4.2. DC conductivity. We present in Fig. 6 the variation of $\sigma_{dc}(T)$ in Arrhenius representation i.e. $\log(\sigma_{dc}) = f(1000/T)$. For low temperatures (lower than 100°C), the conductivity increases by increasing temperature. When temperature exceeds 100°C the conductivity decreases. This temperature corresponds to loss of water as indicated by TGA analyses. The loss of water molecules implies the decrease of proton exchange efficiency causing the decrease of the dc conductivity.

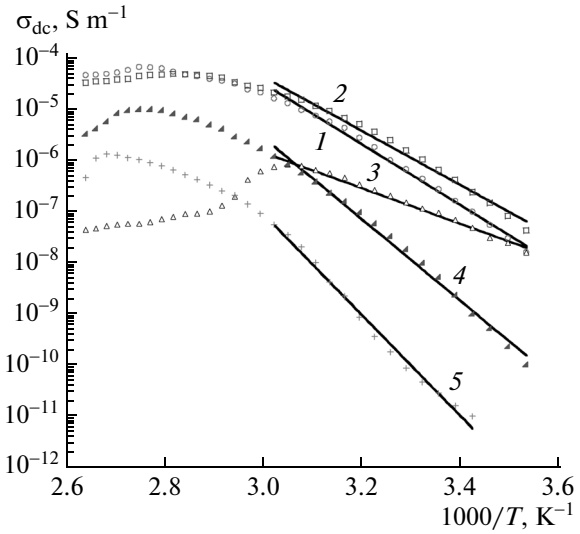

Fig. 6. $\log(\sigma_{dc}) = f(1000/T)$ for (*1*) pure PVA, (*2*) PVA/NH_4Cl 4%, (*3*) PVA/NH_4Cl 16%, (*4*) PVA/$NH_4CH_3CO_2$ 4%, and (*5*) PVA/$NH_4CH_3CO_2$ 12% (solid lines are fitting curves to Arrhenius law).

We fit σ_{dc} to the Arrhenius law given by:

$$\sigma_{dc}(T) = \sigma_0 \exp\left(-\frac{E_a}{k_B T}\right), \quad (3)$$

where E_a is the activation energy, $k_B = 1.38\ 10^{-23}$ J/K the Boltzmann constant, T the absolute temperature and σ_0 a pre-exponential factor. Activation energies are presented in Table 2. We obtain energy values in the order of 1 eV which is convenient with ionic type conductivity in disordered materials [19]. In fact, the activation energy of conductivity in electronic conducting polymers and their composites is situated in the order

Table 2. Activation energies of dc conductivity, conductivity relaxation, alpha relaxation electrode relaxation for pure PVA and various composites

Sample	Activation energy, eV			
	D_c conductivity	conductivity relaxation	α relaxation	interfacial relaxation
Pure PVA	1.18 ± 0.12	1.25 ± 0.12	1.01 ± 0.1	0.89 ± 0.09
PVA/NH_4Cl 4%	1.05 ± 0.1	1.11 ± 0.11	0.82 ± 0.08	0.95 ± 0.09
PVA/NH_4Cl 8%	0.69 ± 0.07	0.59 ± 0.06	0.7 ± 0.07	0.64 ± 0.06
PVA/$NH_4CH_3CO_2$ 4%	1.58 ± 0.16	1.6 ± 0.16	1.42 ± 0.14	1.37 ± 0.14
PVA/$NH_4CH_3CO_2$ 8%	1.95 ± 0.2	2.3 ± 0.23	1.53 ± 0.15	1.84 ± 0.18

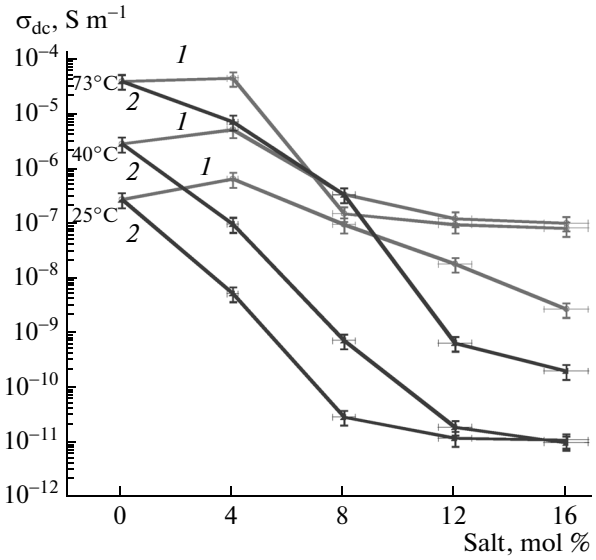

Fig. 7. Variation of σ_{dc} versus salt amount in (*1*) PVA/NH_4Cl and (*2*) PVA/$NH_4CH_3CO_2$ at various temperatures: (*3*) 25, (*4*) 40, (*5*) 73°C.

of meV. As a comparison between the two types of composites at the same salt amount, we obtain higher activation energy with ammonium acetate than with ammonium chloride with values lying around 2 eV; this indicated higher barrier energy values through which the charge carrier will hop. We attribute this result to a crosslinking between the salt and the PVA chains which is a strong interaction reducing the mobility of the charge carrier. This interaction is confirmed by infrared measurements showing the broadening of the hydroxyl absorption band. This result is compatible with the relative higher values of T_g in PVA/ammonium acetate which indicated lower mobility of PVA chains which reduces the ion mobility.

The evolution of the dc conductivity as a function of salt amount is presented in Fig. 7; it shows that with NH_4Cl the conductivity presented the higher value with the composite 4%. Contrarily, with $NH_4CH_3CO_2$ the dc conductivity decreases with the salt amount. In both composites, the evolution of the dc conductivity

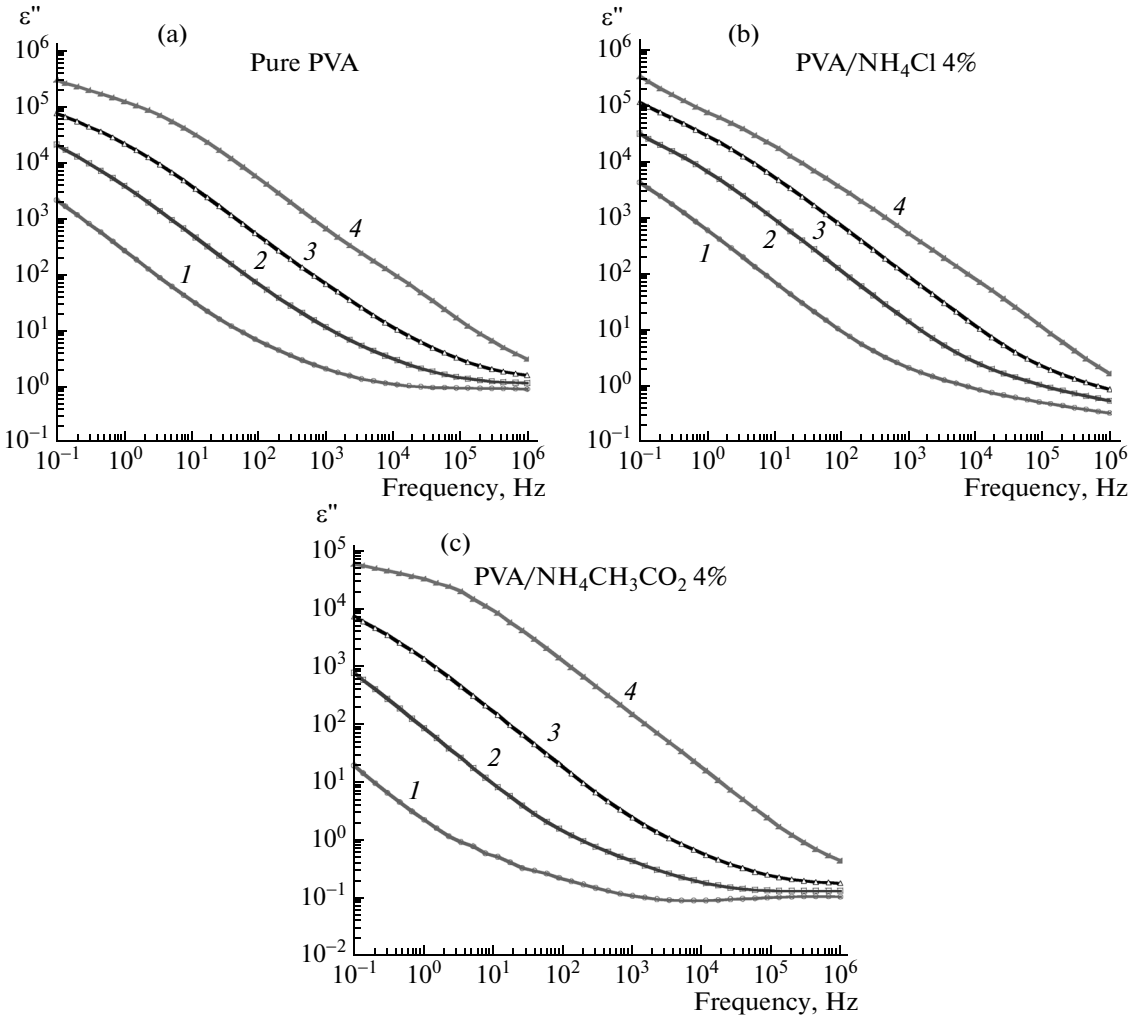

Fig. 8. The global loss factor ε" for (a) pure PVA, (b) PVA/NH_4Cl 4%, and (c) PVA/$NH_4CH_3CO_2$ 4% at various temperatures (*1*) 10, (*2*) 25, (*3*) 40, and (*4*) 70°C (82°C for (c)).

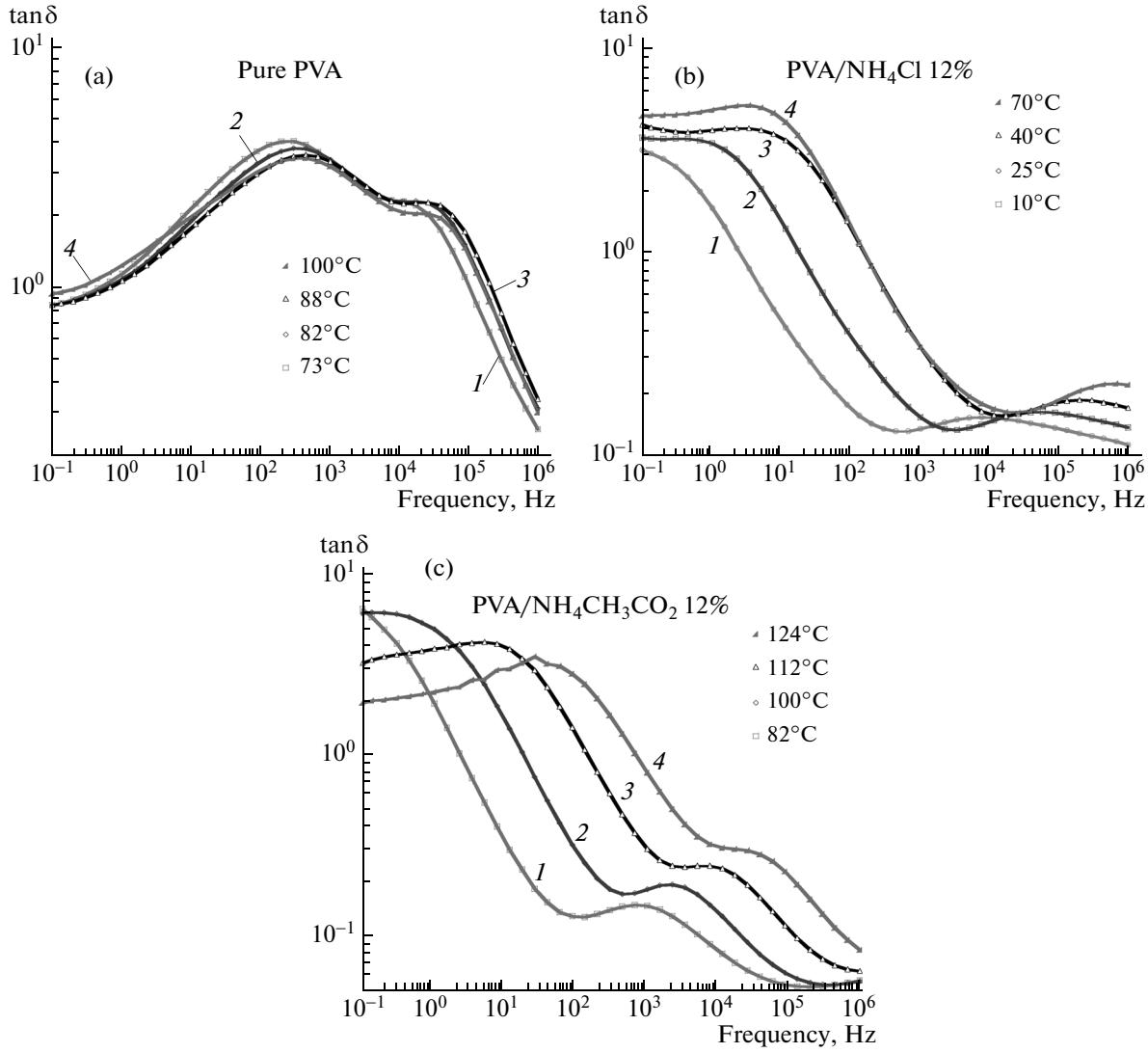

Fig. 9. Angle loss tangent for (a) pure PVA at various temperatures (*1*) 73, (*2*) 82, (*3*) 88, and (*4*) 100°C; (b) PVA/NH_4Cl 4% at various temperatures (*1*) 10, (*2*) 25, (*3*) 40, and (*4*) 70°C; and (c) PVA/$NH_4CH_3CO_2$ 14% at various temperatures (*1*) 82, (*2*) 100, (*3*) 112, and (*4*) 124°C.

goes in the same direction as the evolution of water uptake.

The retained water constitutes a relevant parameter for ionic conductivity enhancement. To prove this presumption, we measured the dc conductivity of films after immersion in pure water by using the 4-points method. Results showed an enhancement of the conductivity by many orders of magnitude [20]. For example, PVA/NH_4Cl 8% passed from 9×10^{-8} to 2.7×10^{-3} S/m, PVA/NH_4Cl 12% passed from 1.8×10^{-8} to 2.4×10^{-2} S/m. PVA/$NH_4CH_3CO_2$ composites show similar enhancement of conductivity after hydration. Water retained in the film ensures dissociation of the salt into its ions and facilitates the exchange of H^+ proton between NH_4^+ ion and H_2O. As a conclusion, salt and retained water amounts are essential parameters and must be considered together to obtain higher values of ionic conductivity of PVA/ammonium salt composites.

Dielectric relaxation. We analyze the dielectric relaxation by using the complex dielectric permittivity defined by:

$$\varepsilon(\omega, T) = \varepsilon'(\omega, T) - i\varepsilon''(\omega, T), \quad (4)$$

where ε' defines the dispersion factor and ε'' defines the global loss factor. In general, the global loss factor is expressed as a sum of three terms [21, 22]:

$$\varepsilon'' = \varepsilon''_{dip} + \varepsilon''_{MW} + \varepsilon''_{c}. \quad (5)$$

They constitute respectively, dipolar, interfacial (Maxwell–Wagner) and conduction loss contribu-

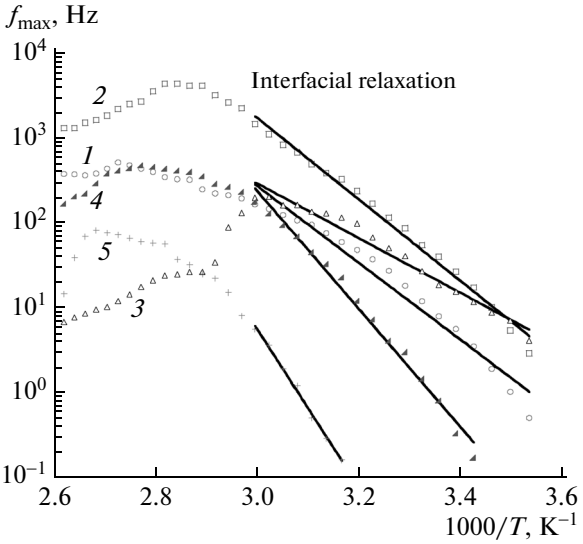

Fig. 10. Variation of $\log(f_{max}) = f(1000/T)$ corresponding to electrode polarization for (*1*) pure PVA, (*2*) PVA/NH_4Cl 4%, (*3*) PVA/NH_4Cl 8%, (*4*) PVA/$NH_4CH_3CO_2$ 4%, (*5*) PVA/$NH_4CH_3CO_2$ 8% composites (solid lines are fitting curves to Arrhenius law).

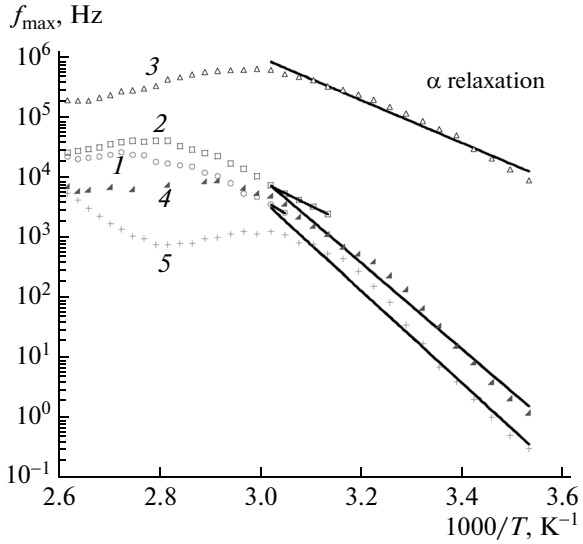

Fig. 11. Variation of $\log(f_{max}) = f(1000/T)$ corresponding to relaxation for (*1*) pure PVA, (*2*) PVA/NH_4Cl 4%, (*3*) PVA/NH_4Cl 12%, (*4*) PVA/$NH_4CH_3CO_2$ 8%, (*5*) PVA/$NH_4CH_3CO_2$ 12% composites (solid lines are fitting curves to Arrhenius law).

tions. The conduction loss factor ε_c'' is defined by [21, 23]:

$$\varepsilon_c'' = \sigma_{dc}/\varepsilon_0\omega \quad (6)$$

To take in account the conductivity and the electrode effects in the dielectric response, it is widely accepted to fit the experimental data of the global loss factor in low frequency region to a power law defined by A/ω^n. If the electrode effect is negligible the exponent n becomes close to 1 and A close to σ_{dc}. This term, proportional to the inverse of the frequency, increases as the frequency decreases. For materials having significant dc conductivity, this term may cause the camouflage of eventual dielectric relaxation peaks expected in the global loss factor curves at low frequencies [21–23].

We present in Figs. 8a, 8b, and 8c $\varepsilon''(\omega)$ curves respectively for pure PVA, PVA/NH_4Cl 4% and PVA/$NH_4CH_3CO_2$ 4% at various temperatures. It is visible that for each temperature, the global loss factor increases as the frequency decreases. This reflects the effect of the conduction loss factor ε_c'', which is inversely proportional to frequency. When we increase temperature the loss factor increases. This agrees with the increase of the dc conductivity with temperature. The two series of composites show similar behavior. But we observe lower loss factor values for PVA/$NH_4CH_3CO_2$ composite compatible with its low conductivity.

We present in Figs. 9a, 9b, and 9c experimental curves of the angle loss tangent defined by: $\tan(\delta) = \frac{\varepsilon''}{\varepsilon'}$ respectively for pure PVA, PVA/NH_4Cl 12% PVA/$NH_4CH_3CO_2$ 12% at various temperatures. ε' and ε'' are obtained from the dielectric measurement as the real and the imaginary parts of the permittivity and represent the dispersion and the global loss factor terms respectively. We localize 1st relaxation peak which appears at low frequencies and when we increase temperature, 2nd relaxation peak appears at relative higher frequencies. We attribute the 1st peak to electrode polarization; it is due to accumulation of charges at the electrode/sample interface. We attribute the 2nd peak to the alpha relaxation corresponding to segmental movements of PVA chains. For each of composites, the relaxation frequency (the frequency of the peak) which we noted f_{max} depends on temperature and depends also on the salt amount in the composite.

We present in Figs. 10 and 11 $\log(f_{max}) = f(1000/T)$ curves corresponding respectively to sample/electrode polarization and alpha relaxation for various PVA composites.

At lower temperatures, the relaxation frequency (f_{max}) increases with temperature but when temperature exceeds 100°C the relaxation frequency decreases. The fitting of experimental data to the Arrhenius law gives activation energies which we presented in Table 2. We found activation energy values in the order of 1 eV which is compatible with dipole orientation/reorientation processes [21–23]. The relaxation frequency of the interfacial mode presents higher values for the samples having higher values of conductivity. Keeping in mind that $f_{max} = 1/\tau$ where τ is the relaxation time, we conclude that faster relaxation

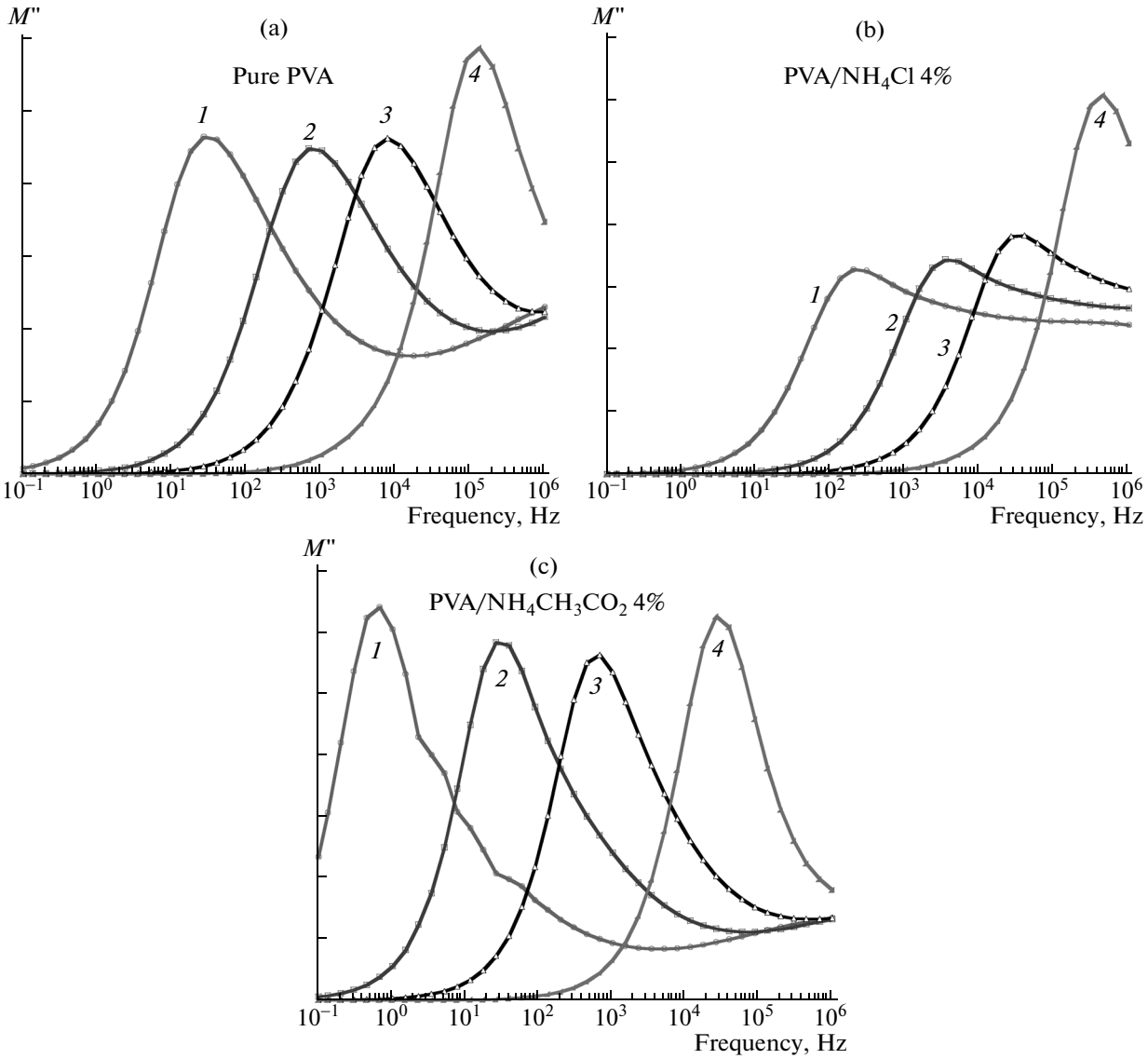

Fig. 12. Imaginary part of the dielectric modulus for pure (a) PVA, (b) PVA/NH_4Cl 4%, and (c) PVA/$NH_4CH_3CO_2$ 4% at (*1*) 10, (*2*) 25, (*3*) 40, and (*4*) 70°C.

process is observed in more conductive samples. Concerning alpha process, the relaxation frequency varies compatibly to the glass transition T_g. When T_g decreases the relaxation frequency increases i.e. the increase of PVA chains mobility decreases the corresponding relaxation time.

We adopt the dielectric modulus defined by:

$$M(\omega, T) = 1/\varepsilon(\omega, T) = M'(\omega, T) + iM''(\omega, T) \quad (7)$$

It is equivalent to $M'(\omega) = \dfrac{\varepsilon'}{\varepsilon'^2 + \varepsilon''^2}$ and $M''(\omega) = \dfrac{\varepsilon''}{\varepsilon'^2 + \varepsilon''^2}$.

Experimental curves of the imaginary part $M''(\omega)$ for pure PVA, PVA/NH_4Cl 4% and PVA/$NH_4CH_3CO_2$ 4% are presented in Figs. 12a, 12b, and 12c respectively. Curves reveal a relaxation peak with a relaxation frequency f_{max} depending on temperature and also on the salt amount. The representation of $\log(f_{max}) = f(1000/T)$ for this relaxation is in Fig. 13.

Curves are similar in shape to that of $\log(\sigma_{dc}) = f(1000/T)$ and the fitting to the Arrhenius law by using the same number of points gives activation energies values close to those obtained for σ_{dc} as exposed in Table 2. We attribute this peak to conductivity relaxation consisting in forward/backward hopping of mobile ions between localization sites randomly distributed in the bulk. In both series, the variation of the relaxation time of this mode versus temperature and versus the salt amount is in good agreement with the

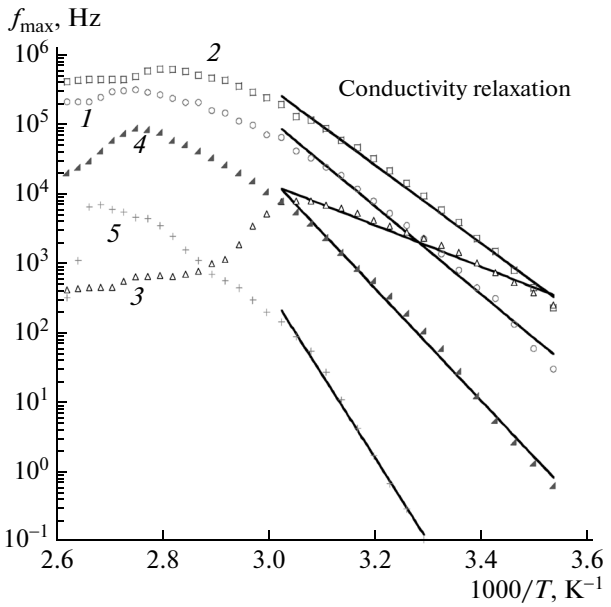

Fig. 13. Variation of $\log(f_{max}) = f(1000/T)$ corresponding to conductivity relaxation for (*1*) pure PVA, (*2*) PVA/NH_4Cl 4%, (*3*) PVA/NH_4Cl 8%, (*4*) PVA/$NH_4CH_3CO_2$ 4%, (*5*) PVA/$NH_4CH_3CO_2$ 8% composites (solid lines are fitting curves to Arrhenius law).

conductivity; shorter relaxation times (i.e. higher relaxation frequencies) are obtained for higher values of conductivity.

CONCLUSIONS

In this work we prepared composite films of polyvinyl alcohol/ammonium chloride and polyvinyl alcohol/ammonium acetate by simple casting aqueous solution. Results showed that retained water enhanced the plasticity of the composite and the salt addition provide a source of protons ensuring the ionic conductivity and enhances the thermal stability. The electric conductivity is enhanced by water uptake. The conductivity in alternative regime is frequency independent in the low frequency range at low temperatures and well described by a power law in the high frequency range. By using the dielectric permittivity and the dielectric modulus we have detected three dielectric relaxation processes attributed to electrode/sample interface polarization, alpha relaxation and conductivity relaxation.

REFERENCES

1. M.-S. Kang, Y.-J. Choi, and S.-H. Moon, J. Membr. Sci. **207**, 157 (2002).
2. J. Malathi, M. Kumaravadivel, G. M. Brahmanandhan, M. Hema, R. Baskaran, and S. Selvasekarapandian, J. Non-Cryst. Solids **356** (43), 2277 (2010).
3. L. E. Karlsson, B. Wesslen, and P. Jannasch, Electrochim. Acta **47** (20), 3269 (2002).
4. K. Nomura and T. Koga, J. Colloid Interface Sci. **241** (2), 428 (2001).
5. J. E. Hensley and J. D. Way, J. Power Sources **172** (1), 57 (2007).
6. B. Smitha, S. Sridhar, and A. A. Khan, J. Membr. Sci. **259** (1–2), 10 (2005).
7. L. Chikh, V. Delhorbe, and O. Fichet, J. Membr. Sci. **368** (1–2), 1 (2011).
8. L. Lebrun, E. D. Silva, and M. Metayer, J. Appl. Polym. Sci. **84** (8), 1572 (2002).
9. D. S. Kim, H. B. Park, J. W. Rhim, and Y. M. Lee, Solid State Ionics **176** (1–2), 117 (2005).
10. A. Chandan, M. Hattenberger, A. El-Kharouf, S. Du, A. Dhir, V. Self, B. G. Pollet, A. Ingram, and W. Bujalski, J. Power Sources **231**, 264 (2013).
11. G. K. Prajapati, R. Roshan, and P. N. Gupta, J. Phys. Chem. Solids **71** (12), 1717 (2010).
12. M. Hema, S. Selvasekarapandian, G. Hirankumar, A. Sakunthala, D. Arunkumar, and H. Nithya, Spectrochimica Acta, Part A **75** (1), 474 (2010).
13. M. Hema, S. Selvasekarapandian, D. Arunkumar, A. Sakunthala, and H. Nithya, J. Non-Cryst. Solids **355** (2), 84 (2009).
14. J.-W. Rhim, H. B. Park, C.-S. Lee, J.-H. Jun, D. S. Kim, and Y. M. Lee, J. Membr. Sci. **238** (1–2), 143 (2004).
15. E. Sheha, N. Mona, and M. K. El-Mansy, Phys. Scr. **88** (3), 035701 (2013).
16. M. K. El-Mansy, E. M. Sheha, K. R. Patel, and G. D. Sharma, Optik **124** (13), 1624 (2013).
17. A. K. Jonscher, *Universal Relaxation Law* (Chelsea Dielectric Group, London, 1996).
18. V. D. Noto, N. Boaretto, E. Negro, and G. Pace, J. Power Sources **195** (23), 7734 (2010).
19. A. L. Saroj, R. K. Singh, and S. Chandra, Materi. Sci. Eng., B **178** (4), 231 (2013).
20. M. Eikerling, J. Phys.: Condens. Matter **23** (23), 230301 (2011).
21. B. G. Soares, M. E. Leyva, G. M. O. Barra, and D. Khastgi, Eur. Polym. J. **42** (3), 676 (2006).
22. A. Fattoum, F. Gmati, N. Bohli, M. Arous, and A. Belhadj Mohamed, J. Phys. D: Appl. Phys. **41** (9), 095407 (2008).
23. A. Fattoum, M. Arous, F. Gmati, W. Dhaoui, and A. Belhadj Mohamed, J. Phys. D: Appl. Phys. **40** (14), 4347 (2007).